Available online at www.sciencedirect.com

ScienceDirect

Energy Procedia 82 (2015) 172 – 179

Energy Procedia

ATI 2015 - 70th Conference of the ATI Engineering Association

HAWT Design and Performance Evaluation: Improving the BEM theory Mathematical Models

R. Lanzafame[a], *S. Mauro**[a], *M. Messina*[a]

[a]*Department of Industrial Engineering, University of Catania, Viale A. Doria, 6 – 95125 Catania, Italy*

Abstract

This paper presents an improved numerical code based on BEM theory, implemented to evaluate the performance of a HAWT (Horizontal Axis Wind Turbines). This numerical code is a 1-D code characterized by fast processing times and reliable results. The critical aspects of the codes based on the BEM theory are widely known in scientific literature. In this paper, the authors explain how to resolve these aspects. One of these is represented by the radial flow along the blades. Radial flow is a 3-D flow, but can be dealt with inside a 1-D code only using a mathematical expedient. This expedient was tested and validated for the Risø test turbine LM 8.2 (with the NACA 63_x-2xx airfoil series along the blades). Radial flow along the blades is taken into account, thus increasing the experimental C_L distribution in the stalled aerodynamic region, based on CFD 3D results. The mathematical equation adopted to describe the C_L distribution of the NACA 63_x-2xx airfoil is a fifth order logarithmic polynomial. With this numerical code, the mechanical power curve of the Risø test turbine has been calculated, and then compared with the experimental curve found in scientific literature.

Peer-review under responsibility of the Scientific Committee of ATI 2015

Keywords: Horizontal Axis Wind Turbine, Blade Element Momentum theory, Wind Turbine Design, Post-Stall Model

* Corresponding author. Tel.: +39-095-7382414; fax: +39 095 337994
E-mail address: mstefano@diim.unict.it

Peer-review under responsibility of the Scientific Committee of ATI 2015
doi:10.1016/j.egypro.2015.12.015

Nomenclature

R	rotor radius [m]	F	tip loss factor [-]
ϑ	twist angle [deg]	C_N	normal force coefficient [-]
α	angle of attack [deg]	λ	tip speed ratio [-]
β	angle of attack shift deg	λ_r	local tip speed ratio [-]
ϕ	incoming flow direction angle [deg]	a_i	twist logarithmic polynomial coefficients
ω	angular velocity [s^{-1}]	b_i	thickness/chord polynomial coefficients
a	axial induction factor [-]	c_i	interpolated chord coefficients
a'	tangential induction factor [-]	d_i, f_i	C_D logarithmic polynomial coefficients
r	blade local radius [m]	T	torque [Nm]
V_0	wind velocity far upstream [m/s]	P	power [W]
N	rotor normal force [N]		
c	airfoil chord [m]	*Abbreviations*	
C_L	airfoil lift coefficient [-]	BEM	Blade Element Momentum
C_D	airfoil drag coefficient [-]	AEP	Annual Energy Production
c_p	power coefficient [-]	AoA	Angle of Attack
c_q	torque coefficient [-]	NREL	National Renewable Energy Laboratory
t	airfoil thickness [m]	1-D	One-dimensional
N_b	number of blades [-]	2-D	Two-dimensional
ρ	air density [kg/m^3]	3-D	Three-dimensional

1. Introduction

Numerical codes based on BEM theory for the design and performance evaluation of Horizontal Axis Wind Turbines are powerful tools for both industry and academy institutions. They are 1-D codes with extremely fast processing times and very reliable results but they have specific critical aspects [1, 2].

These aspects are related to an accurate representation of axial and tangential induction factors; the correct mathematical representation of lift and drag airfoil coefficients and, finally, the radial flow along the blades. The effect of the radial flow is known in literature as centrifugal pumping [9, 17] or Himmelskamp effect [16]. Centrifugal pumping is thus a 3-D effect due to the rotation of the rotor which causes radial flow along the blades [9, 10]. This radial flow slows down the flow detached from the airfoil, causing an increase in airfoil lift. Airfoil experimental data are 2-D and taken from wind tunnel measurements. Moreover, because of rotation, Coriolis and centrifugal forces alter the 2-D airfoil characteristics. This is especially pronounced in stall. Therefore, it is thus often necessary to extrapolate existing airfoil deep stall data to include the effect of rotation [4 - 8]. Within a 1-D numerical code a 3-D effect cannot be directly included. Only with a mathematical artifice is it possible to take this into account.

Thus, the 1-D numerical code becomes quite reliable.

Owing to radial flow along turbine blades, mathematical equations describing lift coefficients must overestimate experimental C_L values within a precise range of angle of attack.

In the reviewed literature, radial flow along a rotating blade is dealt with by increasing CL distribution (see [9,11,12]). Some author have increased C_L values at the end of the attached flow condition (i.e. at the end of the linear trend), while others have increased C_L values in the incipient stall condition. Through a comparison of the empirical assumptions and the use of 3D CFD evaluations [19], the best match with experimental data was obtained by increasing C_L values in the region between incipient and full stall.

2. Numerical codes and wind turbine geometry

The proposed numerical code is a 1-D code for the design of Horizontal Axis Wind Turbines. It has extremely fast processing times and it is highly accurate in numerical simulations. This code is based on Blade Element Momentum (BEM) theory, and can be applied to wind rotor design, and/or the evaluation of its performance. It is a useful tool both for industry and academy institutions, for wind turbine design.

This numerical code can maximize wind rotor power, control the power curve, maximize Annual Energy Production (AEP), and help to develop innovative layouts for wind turbines.

The code has been refined in recent years by comparing wind rotor experimental data obtained in wind tunnels [1] and through field testing [2]. In this paper, experimental data was compared to numerical simulations for the Risø test turbine LM 8.2 [2], using the NACA 63x-2xx airfoil for its three blades.

This comparison with a new airfoil was useful in generalizing the post-stall equation applied within the numerical code.

BEM theory based numerical codes subdivide a wind turbine rotor into annuli of *dr* thickness, as the flow of each sector is not dependent on adjacent circular sector flows [3]. By applying the equations of momentum and angular momentum conservation, for each infinitesimal *dr* sector of the blade, axial force and torque can be defined (Eq. (1) and (2)).

The axial force on the blade element of *dr* width is:

$$dN = \frac{\rho}{2}\,\frac{V_0{}^2(1-a)^2}{\sin^2\phi}\,N_b\left(C_L\cos\phi + C_D\sin\phi\right)c\,dr \tag{1}$$

The torque on the blade element of *dr* width is:

$$dT = \frac{\rho}{2}\,\frac{V_0(1-a)}{\sin\phi}\cdot\frac{\omega r\left(1+a'\right)}{\cos\phi}\,N_b\left(C_L\sin\phi - C_D\cos\phi\right)c\,r\,dr \tag{2}$$

Knowing the lift and drag coefficients (C_L and C_D) is of crucial importance in assessing the forces and torques according to Eq. (1) and (2). The wind rotor geometry is the input within the numerical code in the evaluation of rotor performance.

The numerical stability of the mathematical code depends on tangential and axial induction factors. Equations (3), (4) and (5) report the induction factors implemented inside the numerical code:

For a < 0.4 [3]:

$$a = \frac{1}{\dfrac{4F\sin^2\phi}{\dfrac{c\,N_b}{2\pi\,r_1}\left(C_L\cos\phi + C_D\sin\phi\right)} + 1} \tag{3}$$

while for a ≥ 0.4 [15]:

$$a = \frac{18F - 20 - 3\sqrt{C_N\left(50 - 36F\right) + 12F\left(3F - 4\right)}}{36F - 50} \tag{4}$$

and

$$a' = \frac{1}{2}\left(\sqrt{1+\frac{4}{\lambda_r^{\,2}}a(1-a)}-1\right) \tag{5}$$

where F is the Prandtl Tip Loss Factor, as reported in [9] and [11].

The Risø test turbine LM 8.2 is [2] a three blade rotor with a diameter of 19 meters. The chord is variable along the rotor radius, as are the twist and thickness/chord ratio (see Fig. 1). The NACA 63x-2xx airfoil varies along the rotor radius according to the thickness/chord ratio as well.

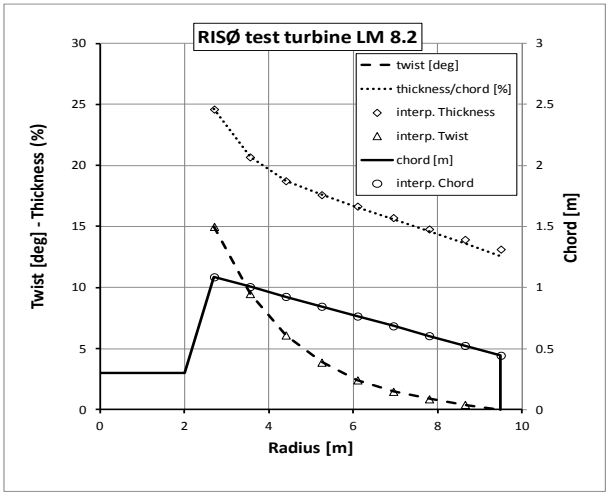

Fig. 1 Risø test turbine geometry

The chord, the twist and the thickness/chord ratio have been interpolated to generate mathematical expressions as geometry input for the code.

The interpolated chord is the linear expression reported in Eq. (6); the interpolated twist is represented by a fifth order logarithmic polynomial (Eq. (7)); the interpolated thickness/chord ratio is a simple fifth order polynomial (Eq. (8)).

$$c(r) = c_1 + c_2 r \tag{6}$$

$$\vartheta(r) = \sum_{i=0}^{5} a_i * [\ln(r)]^i \tag{7}$$

$$t(r)/c(r) = \sum_{i=0}^{5} b_i * r^i \tag{8}$$

The constants of Equations (6), (7) and (8) are reported in Tab. 1.

Tab. 1: Constants of the interpolating equations

Constant	c_1	c_2	a_0	a_1	a_2	a_3	a_4
Value	1.342065359	-0.09450980	89.05442445	-188.801640	210.8086147	-134.641596	44.12243292
Constant	a_5	b_0	b_1	b_2	b_3	b_4	b_5
Value	-5.69888976	77.30100000	-40.4020000	11.31500000	-1.60720000	0.112500000	-0.00310000

3. Numerical code: post-stall model

The airfoil experimental data are 2-D and taken from wind tunnel measurements. Furthermore, because of the rotation of the wind turbine, the boundary layer of the blade is subjected to Coriolis and centrifugal forces which alter the 2-D airfoil characteristics. This is especially pronounced in stall region. It is often necessary, therefore, to modify the 2D airfoil data in order to take into account the rotation effect [4-8].

As seen in literature, many authors modify C_L distribution (see [9, 11, 12, 13]) to take into account radial flow along a rotating blade. In [1, 14] the 2D airfoil characteristics are reported. The data are showed in Fig. 2.

To increase C_L distribution in the stalled region, a new approach was applied. In their past research [18], the authors applied the BEM theory to evaluate the performance of the PHASE VI wind turbine. This wind turbine has two blades with the S809 airfoil. In order to take into account the effect of the centrifugal pumping, the Authors implemented the equation (9) to increase the C_L distribution in the stalled region.

$$C_L = 2C_L\big|_{\alpha=45°} \cdot \sin\alpha \cdot \cos\alpha \tag{9}$$

The use of equation (9) provided a good agreement between simulated and experimental data, better than many other equations used in scientific literature.

In the present work, the wind turbine has the NACA 63_x-2xx airfoil along the blades. As equation (9) does not provide any increase of C_L in the stalled region for this airfoil, the authors have implemented a new mathematical function (the so called polog 2) able to furnish the same C_L increment seen for the S809.

As shown in Figure 2, a linear interpolation was adopted for the 'attached flow condition' ($-8° \leq \alpha \leq 6°$, line curve in Fig. 2), a fifth order logarithmic polynomial for the 'incipient stall condition' ($6° \leq \alpha \leq 20°$, polog curve in Fig. 2), and in the 'fully stalled condition' another fifth order logarithmic polynomial ($20° \leq \alpha \leq 45°$ polog2 curve in Fig. 2).

The characteristics of the polog2 curve are tangency to the experimental data for $\alpha > 50°$ and intersection of the polog curve approximately in the middle of its down-slope. This method provides a suitable increase in C_L (see Fig. 2), allowing the 1-D numerical code to take into account the radial flow along the blades. The proposed correction is verified using 3D CFD simulations as well.

An accurate description of the CFD 3D model was made by the authors in [19]. Summarizing, the model was first generated and calibrated for transitional flows (for a Re of about 1 million) using the NREL PHASE VI HAWT. The computational domain and grid were generated and optimized to obtain independent solutions and meet the requirements of Moving Reference Frame (MRF) and transition turbulence model. The ANSYS Fluent solver was set as a steady state, pressure based, coupled solver, optimizing the turbulence boundary conditions and the Courant number for inner transient sub iterations, so averaging the transient effects as well. The most important feature of the CFD model was the

calibration of the transition turbulence model of Menter for airfoils and wind turbine applications. The power comparison between 1D BEM code, 3D CFD calculations and experimental data for the PHASE VI HAWT is presented in Fig. 3. The good compatibility of the results demonstrates the predictive capabilities of the proposed empirical corrections used in the in-house 1D BEM code.

Similar to the lift coefficient, the drag coefficient data needs to be interpolated. In much the same way, two different mathematical equations are required, one for the attached and incipient stall conditions, another for the fully stalled condition

Consequently, for -8°≤ α ≤20°, a 5th order logarithmic polynomial has been applied (polog1 curve in Fig. 3) (Eq. (10))

$$C_D = \sum_{i=0}^{5} d_i * [\ln(\alpha + \beta)]^i \tag{10}$$

where d_i represents six coefficients derived from experimental data by the least squared method, and β is a shift needed to prevent the logarithm from dropping to '0' or near '0' (30° is a satisfactory value for β to reach a high correlation factor).

For 20°≤ α ≤90° the interpolating function is reported in Equation (11) (*polog2* curve in Fig. 3).

$$C_D = \sum_{i=0}^{5} f_i * [\ln(\alpha + \beta)]^i \tag{11}$$

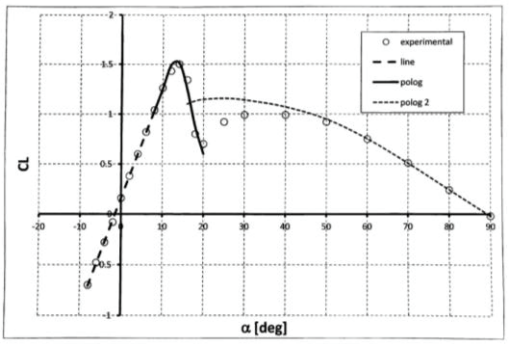

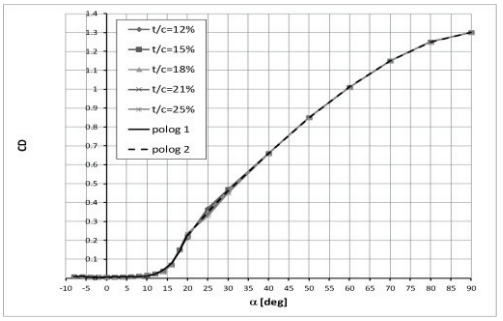

Fig. 2 NACA 63x-2xx airfoil. CL interpolating function for t/c=12% (left) and Drag coefficient interpolation (right)

4. Numerical simulation and experimental validation

By applying the numerical code, a simulated power curve vs wind speed was obtained (see Fig. 3) which represents the mechanical power of the Risø wind turbine LM 8.2 (described in [2]). The numerical simulation was in close proximity to the experimental data, with a maximum error of 6.6 % at a wind speed of 16.5 m/s. The angle of attack varies along the blade at each wind velocity.

Once the wind turbine power (Fig. 3) is evaluated, the torque and power coefficients were obtained (Fig. 4) from Equations (12) and (13).

$$c_p = \frac{P}{\frac{1}{2}\rho\pi R^2 {V_0}^3} \tag{12}$$

$$c_q = \frac{T}{\frac{1}{2}\rho\pi R^3 {V_0}^2} = \frac{c_p}{\lambda} \tag{13}$$

with $\lambda=\omega R/V_0$.

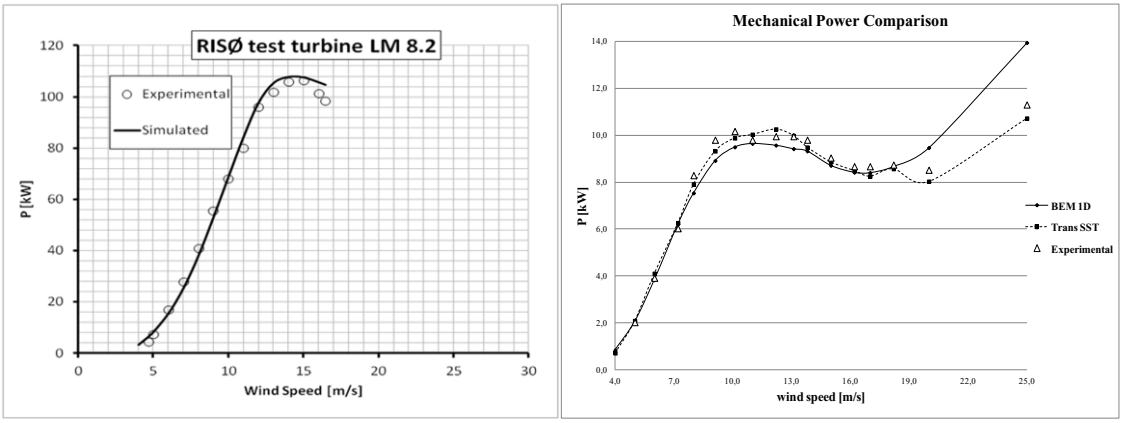

Fig. 3 Comparison between experimental and simulated data for the Risø test turbine (left) and comparison between in-house 1D BEM, Transition CFD 3D and experimental data for the NREL PHASE VI wind turbine [19] (right)

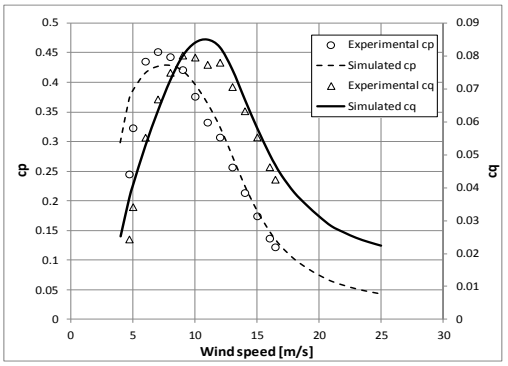

Fig. 4 Torque and power coefficients. Comparison between experimental and simulated data for the Risø wind turbine LM 8.2

Conclusions

In this paper a numerical code for the evaluation of Horizontal Axis Wind Turbine performance was developed, refined and applied. The numerical code is a 1-D numerical code based on BEM theory which is characterized by fast processing times and accurate results. The results are reliable only if the critical aspects of BEM codes are dealt with and resolved. In this work, a Horizontal Axis Wind Turbine was simulated in order to compare experimental and simulated data. The wind turbine is the Risø test turbine LM 8.2 which uses the NACA 63_x-2xx airfoil series. The comparison between experimental and simulated data is critical for the validation of the post-stall model which takes into account the radial flow along the blades. This flow is dealt with by increasing the 2-D airfoil C_L distribution in the incipient

stall/fully stalled aerodynamic regions. The mathematical equations implemented for the lift distribution of the NACA 63_x-2xx airfoils are fifth order logarithmic polynomials.

The numerical code is applied to evaluate mechanical power, power coefficient and torque coefficient. Subsequently, the simulated and experimental data were compared with data found in scientific literature, demonstrating excellent compatibility.

References

[1] Jonkman JM. Modeling of the UAE Wind Turbine for refinement of FAST_AD. NREL/TP-500-34755, December 2003.

[2] J.G. Schepers, A.J. Brand, A. Bruining, J.M.R. Graham, M.M. Hand, D.G. Infield et al. "Final report of IEA Annex XIV : Field Rotor Aerodynamics" –ECN (Energy research Centre of the Netherlands) Report - ECN-C-97-027 - MAY 1997.

[3] Moriarty P.J. and Hansen A.C.: "AeroDyn Theory Manual", Technical Report NREL/TP-500-36881 – January 2005.

[4] M.O.L. Hansena, J.N. Sørensen, S. Voutsinas, N. Sørensen, H.A. Madsen: State of the art in wind turbine aerodynamics and aeroelasticity. Progress in Aerospace Sciences 42 (2006) 285–330. Elsevier Science.

[5] Johansen J, Sørensen NN. Aerofoil characteristics from 3D CFD rotor computations. Wind Energy 2004;7(4):283–94.

[6] Snel H, Houwink B, Bosschers J, Piers WJ, Van Bussel GJW, Bruining A. Sectional prediction of 3-D effects for stalled flow on rotating blades and comparison with measurements. In: Proceedings of the ECWEC 1993, Travemunde, 1993, p. 395–9.

[7] Chaviaropoulos PK, Hansen MOL. Investigating threedimensional and rotational effects on wind turbine blades by means of a quasi-3D Navier–Stokes solver. J Fluids Eng 2000;122:330–6.

[8] Bak C., Johansen J. Three-dimensional corrections of airfoil characteristics for wind turbines based on pressure distributions. In: Proceedings of the EWEC conference, Athens, 27 February–2 March 2006.

[9] Lindenburg C. Investigation into rotor blade aerodynamics. ECN-C-03-025, July 2003.

[10] Bermudez L, Velazquez A, Matesanz A. Viscous–inviscid method for the simulation of turbulent unsteady wind turbine airfoil flow. J Wind Eng Ind Aerodyn 2002;90:643–61.

[11] Corten GP. Flow separation on wind turbine blades. PhD. thesis—Utrecht University, January 2001.

[12] Sphera DA editor. Wind turbine technology: fundamental concepts of wind turbine engineering. 1998.

[13] D. Hu, O. Hua, Z. Du: A study on stall-delay for horizontal axis wind turbine/ Renewable Energy 31 (2006) 821–836.

[14] I.H. Abbott and A.E. Doenhoff Theory of Wing Sections. Dover Publications, Inc, 1958.

[15] Buhl L. Jr. A New Empirical Relationship between Thrust Coefficient and Induction Factor for the Turbulent Windmill State. Technical Report NREL/TP-500-36834 – August 2005.

[16] Himmelskamp, H. 1950, Profiluntersuchungen an Einem Umlaufenden Propeller, Diss. Goettingen 1945, Max-Planck-Inst. fuer Stroemungsforschung, Goettingen, Report No. 2.

[17] Maalawi KY, Negm HN. Optimal frequency design of wind turbine blades. J Wind Eng Ind Aerodyn 2002; 90:961–86

[18] R. Lanzafame, M. Messina - "Fluid Dynamics Wind Turbine Design: Critical Analysis, Optimization and Application of BEM Theory". RENEWABLE ENERGY – Elsevier Science – Vol. 32, (No. 14) November 2007 – pp. 2291 - 2305. ISSN: 0960-1481.

[19] Lanzafame R., Mauro S., Messina M. Wind turbine CFD modeling using a correlation-based transitional model Renewable Energy 52 (2013) 31 - 39 - Elsevier

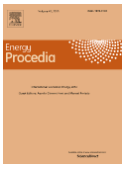

Biography

Stefano Mauro is a Research Fellow at University of Catania. He has a PhD in "Energetic System and Environment". His research mainly deal with CFD, Aerodynamics, Turbulence Modeling, Wind Turbines, Internal Combustion Engine and Fluid Machinery in general. He published 2 works on international journal regarding Wind Turbines CFD modeling.